13th International Symposium on Turbulence and Shear Flow Phenomena (TSFP13)
Montreal, Canada, June 25-28, 2024

Transition to Turbulence on a Concave Surface: Exploring the Effects of Temperature on Görtler Instability

Maher Sawaf
CORIA-UMR 6614 - Normandie Université, CNRS-Université et INSA Rouen-Normandie,
Rouen 76000, France
maher.sawaf@insa-rouen.fr

Mostafa SAFDARI SHADLOO
CORIA-UMR 6614 - Normandie Université, CNRS-Université et INSA Rouen-Normandie,
Rouen 76000, France
mostafa.safdari-shadloo@insa-rouen.fr

Abdellah Hadjadj
CORIA-UMR 6614 - Normandie Université, CNRS-Université et INSA Rouen-Normandie,
Rouen 76000, France
ahadjadj@insa-rouen.fr

Sébastien Poncet
Université de Sherbrooke,
Mechanical Engineering Department
Sherbrooke J1K 2R1, Canada
Sebastien.Poncet@usherbrooke.ca

Stéphane Moreau
Université de Sherbrooke,
Mechanical Engineering Department
Sherbrooke J1K 2R1, Canada
Stephane.Moreau@USherbrooke.ca

ABSTRACT

This study extends the investigation initially conducted by Méndez et al. [1] regarding the laminar-to-turbulent transition process over a concave surface driven by centrifugal instabilities, namely Görtler vortices. In the original study, the transition was meticulously examined through direct numerical simulations (DNS). This work aims to validate these findings by means of Large Eddy Simulations (LES). Furthermore, it examines the influence of wall heat transfer on the transition process by applying the Boussinesq approximation within the allowable temperature range, and also forcing the spanwise wavelength of the perturbation responsible for the transition. This methodology enables the isolated examination of the fundamental impact of temperature gradient on Görtler vortex structures. Specifically, three distinct cases are explored: an adiabatic wall conditions, heating the wall by 60 Kelvin, and cooling the wall by 60 Kelvin. The results demonstrate a nuanced effect of wall temperature on the onset of transition. The heating case leads to a slightly earlier transition, while the cooling condition marginally delays it. However, the most profound impact is observed in the behaviour of secondary instabilities and the mechanisms driving their growth and breakdown.

1 INTRODUCTION

The study of fluid dynamics has long been enriched by exploring Görtler instability and its interactions with heat transfer. Over several decades, researchers have extensively studied how these vortices influence various fluid dynamics scenarios, with a particular focus on heat transfer aspects.

This flow instability, first identified by Görtler in the early 20th century [2], pertains to the formation of streamwise vortices in boundary layers over concave surfaces, influenced by centrifugal forces. Görtler's seminal work in 1940 laid the foundation for studying centrifugal instabilities, focusing on the conditions under which these vortices would manifest in laminar flows over curved surfaces. Görtler's foundational work was primarily theoretical, focusing on the instability mechanisms leading to the formation of vortices in boundary layers over concave surfaces. Görtler analysed the stability of a steady, laminar boundary layer over a concave surface, demonstrating the presence of centrifugal eigenmodes – now known as Görtler vortices. These counter-rotating streamwise structures evolve within the boundary layer, potentially leading to transition if not mitigated. While this study did not directly address the effects of wall temperature or heat transfer, it established the basic principles necessary for understanding how Görtler vortices could be influenced by additional factors, including thermal gradients, in later research.

The study of heat transfer in the context of Görtler vortices initially treated temperature as a passive scalar, examining how they influence the behaviour of heat transfer. In the 1990s, Hall [3] extended the analysis of Görtler vortices by incorporating the effects of thermal stratification in the stability of laminar flows over curved surfaces, proposing a theoretical framework for considering temperature as a factor in the analysis of flow instabilities, and providing insights into how temperature distributions could alter the stability of the flow, yet still primarily viewed temperature as a secondary factor to the mechanical aspects of the instability. As computational capabilities and theoretical models evolved, researchers began to examine temperature not just as a byproduct of fluid motion but as an active participant in the dynamics of flow instabilities, Swearingen and Blackwelder [4] employed experimental techniques to visualize the impact of heat transfer on Görtler instability, highlighting the potential for thermal control strategies in managing flow transitions. Their work underscored the dual role of temperature in both inducing and modulating the characteristics of the vortices. In the realm of numerical simulations, recent studies have leveraged advanced computational fluid dynamics (CFD) tools to dissect the intricate mechanisms by which thermal effects influence Görtler instability. Yang and Zhang's [5] exploration on a flat plate, simulating airflow conditions over the wing of a solar UAV, revealed that a 60 K temperature difference significantly amplifies the drag coefficient, nearly tripling it compared to scenarios without temperature variation. This finding illuminates the profound impact of thermal gradients on sub-boundary layer vortical structures, urging a deeper examination

of how pressure gradients and surface curvature influence the stability of buoyancy driven Görtler vortices, aligning insights more closely with real-world industrial applications. Furthering this discourse, Kametani and Fukagata [6] engaged in a direct numerical simulation (DNS) of a zero-pressure gradient, spatially developing boundary layer, subject to uniform heating and cooling. Their investigation into the mechanisms behind drag reduction/augmentation shed light on the significant drag reduction capabilities of uniform cooling, while uniform heating was found to increase drag. These outcomes highlight the balance between thermal conditions and aerodynamic performance.

Méndez et al .[1] capitalized on the wall roughness perturbation method to achieve a more distinct spanwise characterization of transitional flow, particularly highlighting differences at upwash and downwash locations. This methodological choice diverges from the complexities induced by inlet free-stream turbulence, which could generate overlapping Görtler vortices of multiple wavelengths. This underscores the necessity for a focused study that incorporates temperature as an active scalar, aiming to isolate the characteristics of sub-boundary layer streaks and their dynamics, thereby facilitating a deeper understanding of the fundamental effect of temperature gradients on Görtler vortices.

2 NUMERICAL METHOD

The numerical simulations are performed using commercial Large Eddy Simulation (LES) package, to resolve the large-scale structures of the flow while modeling the smaller, sub-grid scales. The LES formulation employs the Wall-Adapting Local Eddy-viscosity (WALE) [7] model to accurately represent the turbulent stresses, particularly near walls.

2.1 MATHEMATICAL MODELING

The incompressible Navier-Stokes equations, filtered for LES, are given by:

$$\nabla \cdot \bar{\mathbf{u}} = 0 \tag{1}$$

$$\frac{\partial \bar{u}_i}{\partial t} + \bar{u}_j \frac{\partial \bar{u}_i}{\partial x_j} = -\frac{1}{\rho}\frac{\partial \bar{p}}{\partial x_i} + \nu \frac{\partial^2 \bar{u}_i}{\partial x_j \partial x_j} - \frac{\partial \tau_{ij}}{\partial x_j} + f_{b,i} \tag{2}$$

where $\bar{\mathbf{u}}$ is the filtered velocity field, $\bar{p}$ is the filtered pressure field, ν is the kinematic viscosity, and τ_{ij} are the sub-grid scale (SGS) stresses represented by the WALE model. The term $f_{b,i}$ represents the buoyancy force, modeled using the Boussinesq approximation, which is expressed as:

$$f_{b,i} = -\beta(T - T_{\text{ref}})g_i \tag{3}$$

Here, T is the temperature field, T_{ref} is the reference temperature, β is the thermal expansion coefficient, and g_i is the gravitational acceleration component in the i-th direction. The WALE model is implemented to account for the sub-grid scale turbulence and is given by:

$$\tau_{ij} - \frac{1}{3}\tau_{kk}\delta_{ij} = -2\rho\nu_t S^*_{ij} \tag{4}$$

$$\nu_t = \left(\frac{(S^*_{ij}S^*_{ij})^{3/2}}{(\bar{S}_{ij}\bar{S}_{ij})^{5/2} + (S^*_{ij}S^*_{ij})^{5/4}}\right)(C_w\Delta)^2 \tag{5}$$

where ν_t is the sub-grid scale eddy viscosity, $\bar{S}_{ij}$ is the resolved strain-rate tensor, S^*_{ij} is the traceless symmetric part of the square of the velocity gradient tensor, Δ is the filter width, and C_w is a model constant. The convection and diffusion of the temperature field are governed by the filtered energy equation, also modified to account for sub-grid scales:

$$\frac{\partial \bar{T}}{\partial t} + \bar{u}_j \frac{\partial \bar{T}}{\partial x_j} = \alpha \frac{\partial^2 \bar{T}}{\partial x_j \partial x_j} + \frac{\partial q_j}{\partial x_j} \tag{6}$$

where $\bar{T}$ is the filtered temperature field, α is the thermal diffusivity, and q_j represents the sub-grid scale heat flux.

The spatial discretization of the governing equations employs the MUSCL third-order upwind scheme for the convective terms, ensuring high-resolution capturing of flow features. The diffusive terms are discretized using a central differencing scheme.

The segregated flow is used to handle the coupling. The flow and thermal fields are resolved using segregated algorithms. The solver decouples the velocity and pressure fields using a prediction-correction approach, and the temperature field is solved separately, in an iterative manner until satsfactory level of convergance is achieved at each time step. Implicit second-order time integration is utilized to enhance the temporal accuracy of the unsteady simulation. The time step size is chosen based on the Courant-Friedrichs-Lewy (CFL) condition to ensure numerical stability.

2.2 DOMAIN AND BOUNDARY CONDITIONS

Figure 1 shows concave domain with curvature $R = 1\ m$, to allow the balsius profile applied at the inlet to develop into fully turbulent flow . The spanwise length of the domain is wide enough to accomodate 4 sinosoidal roughness elements near the inlet with wavelength λ = 12 mm. This perturbation wavelength ensures maximum growth of instability according to LST.

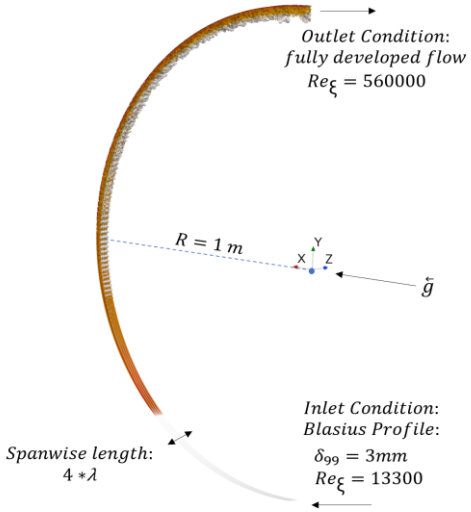

Figure 1: Domain setup, Re_ξ Reynolds number.

3 VALIDATION AND RESULTS

Three cases were examined, a baseline case with adiabatic wall condition to be validated with Mendez's earlier work [1] and two non adiabatic cases in which the wall temperature was raised by 60 Kelvin and lowered by 60 kelvin. The boundary layer's response to the imposed sinusoidal perturbation and temperature gradient is quantitatively depicted through variations in δ^* and θ in Figure 2 and Figure 3 respectively. These boundary layer parameters are critical for identifying the regions of laminar, transitional, and fully turbulent flow. The LES simulation results are presented with the high-fidelity DNS results obtained from the NEK5000 Mendez et al.[1] and the theoretical solutions of the laminar and turbulent boundary layer.

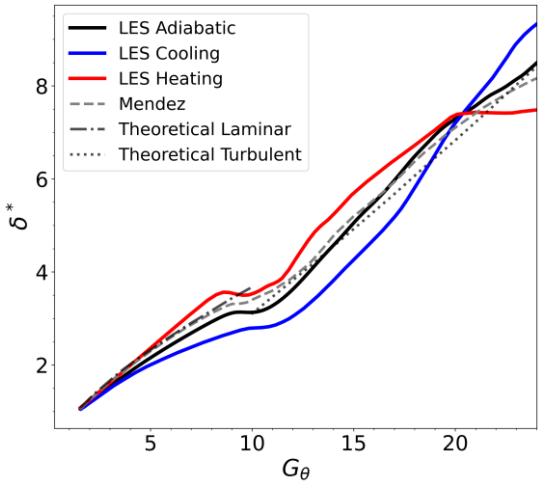

Figure 2: Comparison of spanwise averaged displacement thickness (δ^*) as a function of the Görtler number (G_θ), contrasting LES results with NEK5000 DNS data.

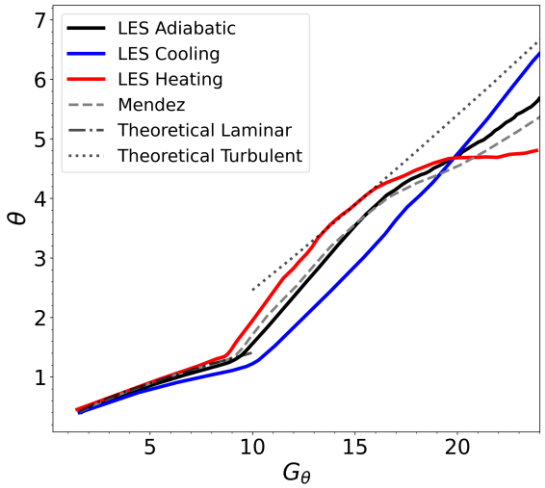

Figure 3: Comparison of spanwise averaged momentum thickness (θ) as a function of the Görtler number (G_θ), contrasting LES results with NEK5000 DNS data.

The LES in the adiabatic case follows Mendez's results and the theoretical solutions available for flat plate. Adding buoyancy effect modified the displacement and momentum thicknesses along the concave domain in a way that they increased when the wall normal vector is in the opposite direction of gravity vector and decreased when it is perpendicular to it.

The transition zone is characterized by a complex interplay between the amplifying Görtler vortices and the destabilizing effects of the perturbations and potentially the temperature gradients in the precense of centrifugal forces.

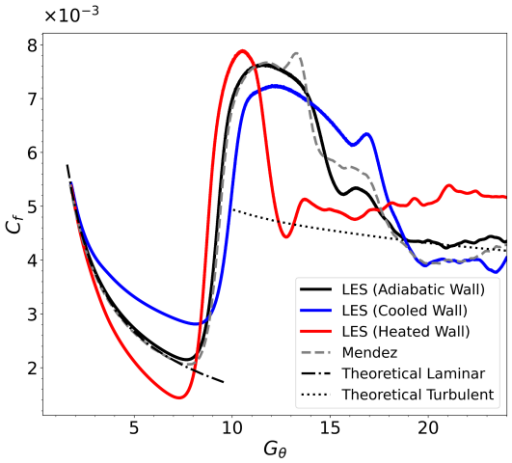

Figure 4: portrays the spanwise averaged skin friction coefficient C_f obtained from the LES alongside the DNS data.

The LES results (all three cases) exhibit this transition, with C_f values decreasing initially following the expected laminar patterns, reaching a minimum that marks the critical Görtler number, G_θ^{cr}, and then increasing again as the flow enters the secondary phase of transition before it goes down again and settle in the fully turbulent region Figure 4. This behavior is a hallmark of the Görtler vortex-induced transition process. In an adiabatic setting, the LES traces a transition pathway where C_f diminishes with increasing G_θ , signifying a prevailing laminar flow regime. As the Görtler number ascends after $G_\theta^{cr} = 8$, a pronounced rise in C_f marks the onset of secondary instabilities, culminating in breakdown to turbulence. Introducing temperature gradient modifies the transition dynamics. Cooling the wall prolongs the laminar state, as indicated by the lower C_f values over an extended G_θ span. This suggests a stabilizing effect of the cooler surface, which suppresses the growth of instabilities. It also prolongs significantly the life of Görtler structures by slowing down the breakdown of secondary instability to full turbulence. Conversely, heating the wall precipitates the transition. The LES shows an earlier increase in C_f bringing G_θ^{cr} down slightly, and denoting a more rapid emergence of instabilities and an accelerated progression to turbulence. the significant event here was the secondary instability again as it breaks down to turbulence very rapidly. This behavior is aligned with the concept that elevated wall temperatures can destabilize the flow, hastening the transition process.

The characterization of instabilities, such as Görtler vortices, is fundamental to understanding the transition from laminar to turbulent flow over curved surfaces. In this context, we analyze the upwash and downwash velocity profiles in adiabatic conditions and observe how thermal effects, namely cooling and heating, alter these profiles. Under adiabatic conditions, the velocity profiles exhibit a clear distinction between the upwash and downwash regions, the upwash is characterized by an acceleration of the fluid particles away from the wall, leading to a thicker boundary layer, while the downwash indicates a deceleration and thinning of the boundary layer. Notably, with increasing Görtler number (G_θ), there is a pronounced growth in the thickness of the upwash region, and an inflectional velocity profile starting from G_θ= 10 indicating low velocity flow far from the wall is carried over high velocity flow near the wall signifying a substantial deviation from the Blasius profile.

Figure 5 (a) compares those profile to Mendez NEK 5000 solution. The downwash region Figure 5 (b) is characterised by boundary layer depression and inflectional profile appearing further downstream at G_θ= 12.
While the general trend of velocity profiles in both upwash and downwash regions were captured with good degree of agreement, it became evident that the meshing can be improved further near the edge of the boundary layer starting at G_θ= 10 in the region where the sudden jump of velocity takes place.

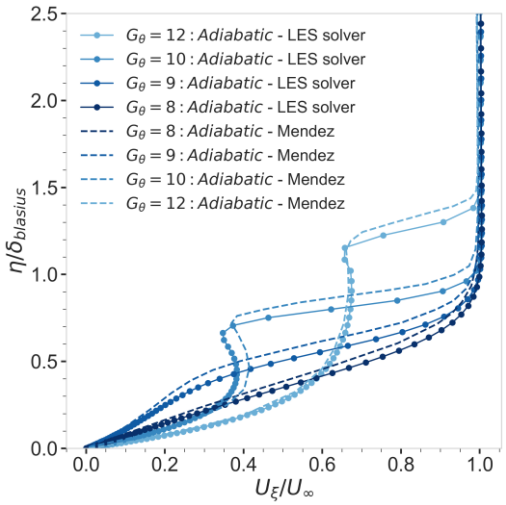

(a): Upwash

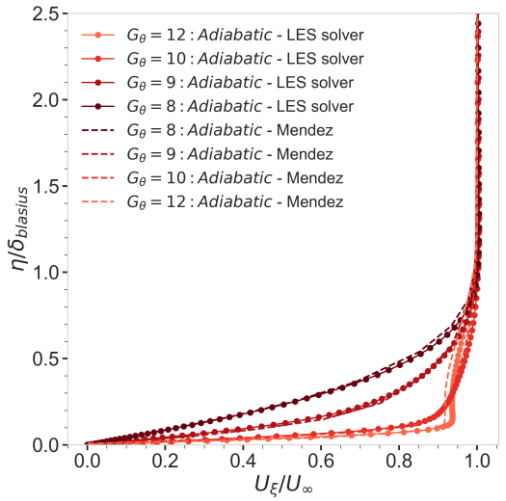

(b): Downwash

Figure 5: Normalized streamwise velocity.

Upon introducing thermal effects, the velocity profiles are noticeably altered, Cooling seems to stabilize the boundary layer, reducing the thickness variations across different Görtler numbers. This effect of cooling down the wall resulted in delaying the inflectional velocity profile from G_θ= 10 in the adiabatic condition to G_θ= 12. An inflectional velocity profile, where the second derivative of the velocity with respect to the spatial coordinate changes sign, inherently lacks the damping effect of viscosity on perturbations. According to Rayleigh's inflection point criterion, such profiles are susceptible to inviscid instabilities.
This susceptibility arises because inflection points allow for the concentration of vorticity at specific layers within the flow, which can amplify small disturbances rather than dissipate them. Consequently, the presence of an inflection point in the velocity profile can lead to an increased likelihood of the flow transitioning to turbulence, as these amplified disturbances grow and lead to chaotic, non-linear flow behaviors.
In contrast, heating exacerbates the boundary layer growth with downwash and upwash streamwise velocity profiles both resembling a profile of turbulent boundary layer at G_θ = 12 Figure 6. Inflectional velocity profile in heating condition shifts upstream to G_θ = 9 indicating energized distrurbance signal thereby enhancing the instability. This thermal effect accelerates the transition to turbulence, particularly as it leads to a more pronounced or additional inflection points in the velocity distribution as shown in G_θ= 12 where multiple inflections are apparent.
Turbulence in boundary layers is profoundly affected by thermal conditions. The Reynolds stresses, representing turbulent momentum fluxes, are key to understanding these effects. This study analyzes the normalized mean velocity profile (U^+) and the Reynolds stresses under adiabatic, heating, and cooling conditions. Figure 7 presents the U^+ profile compared to the classical law of the wall. LES data at G_θ= 23.8 in the adiabatic setting adheres closely to the viscous sublayer and logarithmic layer, validating the LES model's ability to replicate turbulent boundary layer flow.

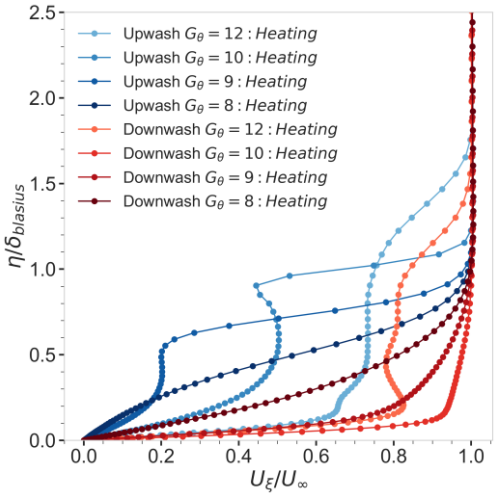

Figure 6: Heating condition, normalized streamwise velocity.

Upon examining the U^+ versus Y^+ plot, it is apparent that the cooling (blue curve) and heating (red curve) of the wall exert distinct influences on the turbulent boundary layer. Counterintuitively, the cooled wall exhibits higher U^+ values, indicating an enhancement in turbulent kinetic energy near the wall, an observation that agrees well with findings from Figures 2 to 4 where the characteristics of δ^* , θ and C_f respectively reverse as the orientation of surface normal with respect to gravity vector changes from opposite in the middle of the domain to perpendicular near the outlet at G_θ= 23.8. thus δ^* , θ in cooling condition decrease compared to adiabatic condition while they increase significantly in the fully turbulent region near the outlet in a complete reversal of behaviour explained by the curvature of the domain changing the bouyancy effect and the way it desturbs the flow.
The heated wall shows lower U^+ values, suggesting a reduction in turbulence intensity or alterations in the turbulent structures, potentially due to the aforementioned curvature of the domain. These observations underscore the complex relation between thermal effects and turbulent flow dynamics, especially in the context of a concave surface.
In comparison against Mendez results [1] in the adiabatic condition Figure 8. Notable is the peak in wall-normal stresses

($\langle u'u' \rangle / u_\tau^2$) and the asymmetric profile of Reynolds shear stress ($\langle u'v' \rangle / u_\tau^2$), indicative of the complex turbulent structures within the flow were all captured perfectly especially at lower Y^+ values. A small deviation at larger Y^+ indicative of inadequate meshing in those regions.

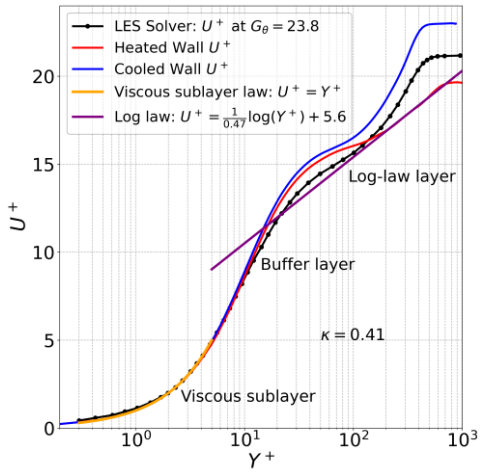

Figure 7: Normalized mean velocity profile U^+ compared with the viscous sublayer and log-law.

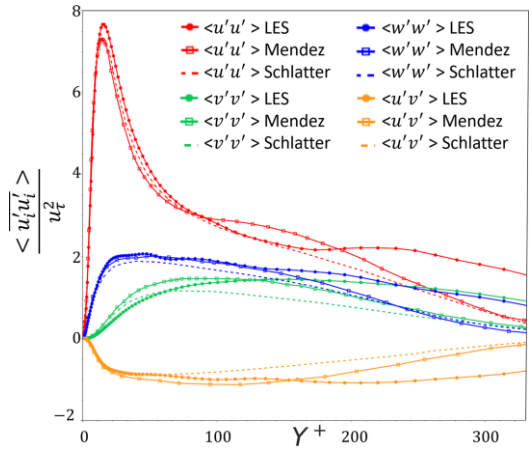

Figure 8: Normalized reynolds stresses.

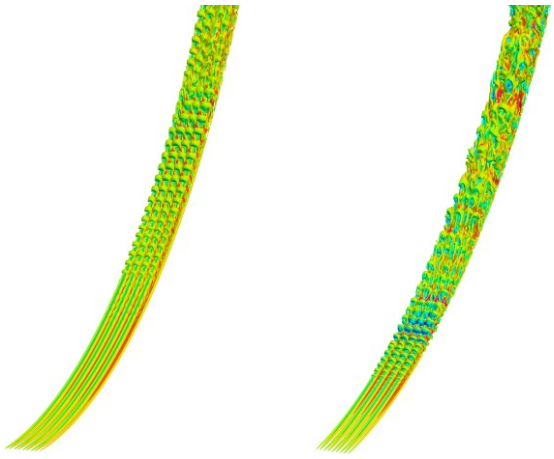

(a) (b)

Figure 9: Vortical structures at $Q = 200\, s^{-2}$ colored by contours of normalized radial velocity V_η (a) cooling condition and (b) heating condition.

The examination of Görtler rolls evolution in both heating and cooling conditions Figure 9, Q criterion visualziation shows the remarkable discrepancy between both cases. Cooling down the wall has resulted in a slight delay in initiation of the primary rolls. Neverthless it extended the life of secondary instability which manifests itself as a wavy pattern in the streamwise direction on top of the roll at each side, later on they inch closer and touch to form the horseshoe structure. Heating the wall significantly shortened the life of secondary instability causing the horseshoe structure to breakdown to turbulence very quickly.

The onset of turbulence is fundamentally marked by the evolution of secondary instabilities, which are significantly influenced by the thermal boundary conditions at the wall, underscored by the gradients of the velocity components in the streamwise (θ) and radial (η) directions under adiabatic and heated wall conditions. Yu et al. [8] in their study on the mechanism of sinuous and varicose modes in secondary instability of Görtler rolls implied that the axial gradient of streamwise velocity $\frac{\partial V_\theta}{\partial z}$ is responsible for the transformation of primary Görtler vortices to the horseshoe structure. in heating scenario the horseshoe structure grows much faster and breakdowns to what resembles a turbulent state very early. Figure 10 shows quick distortion of $\frac{\partial V_\theta}{\partial z}$.

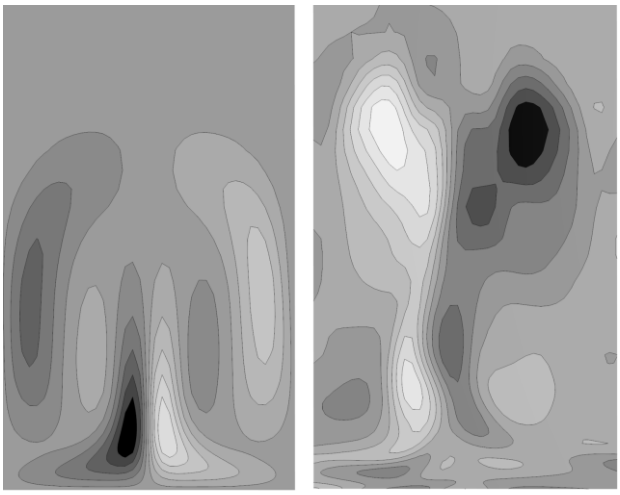

Figure 10: Gradient of streamwise velocity, $\frac{\partial V_\theta}{\partial z}$, under heating, revealing disturbances that precede the rapid transition to turbulence.

Adding buoyancy to the flow as in heating case has resulted in high rotation of the axial gradient of the radial velocity $\frac{\partial V_\eta}{\partial z}$ to such an extent the flow is destined to an immediate breakdown to turbulence. Figure 11 shows when the wall is heated this rotation in $\frac{\partial V_\eta}{\partial z}$ appears very early at G_θ= 11 resulting in breaking the horseshoe structure immediately past that streamwise lcoation. For the adiabatic wall case, the axial shear in streamwise velocity, quantified by $\frac{\partial V_\theta}{\partial z}$, exhibits rotation at elevated Görtler numbers. This shear rotation is the precursor to the formation of the secondary instability, which manifest itself as growing perturbations in the streamwise direction of the vortical structures leading to the formation of horseshoe structures. These events spatially grow until the rotation of $\frac{\partial V_\eta}{\partial z}$

just before full breakdown to turbulence. In heated wall scenario the buoyancy force in the presence of centrifugal force and growing perturbation rotates $\frac{\partial V_\eta}{\partial z}$ very rapidly and very early resulting in shortening of the secondary instability and early breakdown to full turbulence. Cooling the wall down has reverse effects leading to the significant prolongation of the secondary instability.

The buoyancy effect acts to augment the centrifugal forces within the flow. It results in a pronounced radial velocity gradient in the axial direction that rotates and can become so steep that the associated shear layer becomes unstable. The perturbations caused by this steep gradient and the instability of the shear layer interact with the Görtler vortices, energizing them and accelerating the transition from laminar to turbulent flow. Consequently, the superimposed effects of buoyancy-driven instabilities and centrifugal forces culminate in a rapid and earlier onset of turbulence.

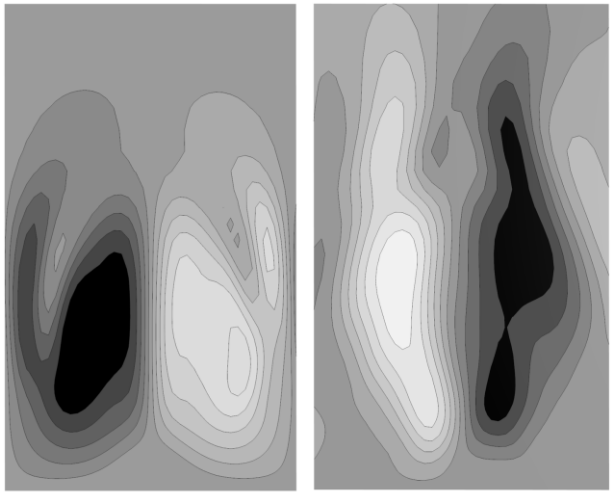

$\frac{\partial V_\eta}{\partial z}\ at\ G_\theta = 11$ $\frac{\partial V_\eta}{\partial z}\ at\ G_\theta = 12$

Figure 11: Gradient of radial velocity, $\frac{\partial V_\eta}{\partial z}$, under heated wall conditions, showing an earlier rotation at $G_\theta = 11$, before the early onset of full turbulence.

4 CONCLUSIONS

The study investigates the influence of wall temperature on the transition dynamics of boundary layer flow over a concave surface. It reveals that temperature variations significantly alter the transition onset and subsequent turbulence breakdown. Specifically, wall heating accelarates the transition, whereas cooling delays it. The transitional region experiences the most significant impact from the prolongation of instabilities before transitioning to full turbulent flow under cooling conditions, whereas heating accelerates this process spatially.

The axial shear of radial velocity, $\frac{\partial V_\eta}{\partial z}$, plays a crucial role in indicating the onset of turbulence. Notably, a pronounced rotational change occurs at Görtler number $G_\theta = 11$ for the heated wall, suggesting a quicker turbulence breakdown compared to the adiabatic case, where this change manifests later at $G_\theta = 13.5$. Furthemore, the study confirms that wall temperature affects the growth of momentum and displacement thickness, with heating causing an increase and cooling resulting in a decrease, this behaviour reverses when the wall normal vector becomes perpendicular to gravity direction. These findings offer valuable insights for thermal effects and turbulent mixing in aerodynamic applications, emphasizing the subtile balance between thermal conditions, pressure gradients, and flow stability.

AKNOWLEDGEMENT

The authors acknowledge the financial support of the French Agence Nationale de la Recherche and LabEx EMC3 through the project FIRST (Grant No. 10-LABX-0009).

The authors acknowledge the access to French HPC resources provided by the French regional computing center of Normandy (CRIANN) (grant nu: 2017002).

REFERENCES

[1] Méndez, M., Safdari Shadloo, M., & Hadjadj, A. (2020). Heat-transfer analysis of a transitional boundary layer over a concave surface with Görtler vortices by means of direct numerical simulations. Physics of Fluids, 32(7).

[2] Görtler, H. (1940). Über den Einfluss der Wandkrümmung auf die Entstehung der laminaren Grenzschicht [On the influence of wall curvature on the formation of the laminar boundary layer]. Nachrichten der Akademie der Wissenschaften in Göttingen, Mathematisch-Physikalische Klasse, IIb, 1, 1-21.

[3] Hall, P., & Fu, Y. (1993). Effects of Görtler vortices, wall cooling and gas dissociation on the Rayleigh instability in a hypersonic boundary layer. Journal of Fluid Mechanics, 247, 503-525.

[4] Swearingen, J. D., & Blackwelder, R. F. (1987). The growth and breakdown of streamwise vortices in the presence of a wall. Journal of Fluid Mechanics, 182, 255-290.

[5] Wang, M., Ma, D., & Zhang, L. (2023). Numerical Study on Buoyancy-Driven Görtler Vortices above Horizontal Heated Flat Plate. Aerospace, 10(685).

[6] El Amrani, S. (2018). The Effect of Wall Cooling and Heating on Görtler Vortices in High-Speed Boundary Layers. Theses and Dissertations, 4383.

[7] Kamali Moghadam, Ramin, Khodayar Javadi, and Farzad Kiani. "Assessment of the LES-WALE and zonal-DES turbulence models in simulation of the flow structures around the finite circular cylinder." Journal of Applied Fluid Mechanics 9.2 (2016): 909-923.

[8] Yu, X., & Liu, J. T. (1994). On the mechanism of sinuous and varicose modes in three dimensional viscous secondary instability of nonlinear Görtler rolls. Physics of Fluids, 6(2), 736-750.